Available online at www.sciencedirect.com
SCIENCE DIRECT®
Geochimica et Cosmochimica Acta 70 (2006) 1322–1335
Geochimica
www.elsevier.com/locate/gca

The influence of carbon on trace element partitioning behavior

Nancy L. Chabot [a,*], Andrew J. Campbell [b,1], John H. Jones [c], Munir Humayun [d], H. Vern Lauer Jr. [e]

[a] Johns Hopkins Applied Physics Laboratory, 11100 Johns Hopkins Road, Laurel, MD 20723, USA
[b] Department of the Geophysical Sciences, The University of Chicago, 5734 S. Ellis Ave., Chicago, IL 60637, USA
[c] Mail Code KR, NASA Johnson Space Center, Houston, TX 77058, USA
[d] National High Magnetic Field Laboratory, Department of Geological Sciences, Florida State University, Tallahassee, FL 32310, USA
[e] ESCG/Barrios Technology, P.O. Box 58477, Houston, TX 77258, USA

Received 14 June 2005; accepted in revised form 10 November 2005

Abstract

Carbon has been proposed as a potential light element in planetary cores, included in models of planetary core formation, and found in meteoritic samples and minerals. To better understand the effect of C on the partitioning behavior of elements, solid/liquid partition coefficients (D = (solid metal)/(liquid metal)) were determined for 17 elements (As, Au, Co, Cr, Cu, Ga, Ge, Ir, Ni, Os, Pd, Pt, Re, Ru, Sb, Sn, and W) over a range of C contents in the Fe–Ni–C system at 1 atm. The partition coefficients for the majority of the elements increased as the C content of the liquid increased, an effect analogous to that of S for many of the elements. In contrast, three of the elements, Cr, Re, and W, were found to have anthracophile (C-loving) preferences, partitioning more strongly into the metallic liquid as the C content increased, resulting in decreases to their partition coefficients. For half of the elements examined, the prediction that partitioning in the Fe–Ni–S and Fe–Ni–C systems could be parameterized using a single set of variables was not supported. The effects of S and C on elemental partitioning behavior can be quite different; consequently, the presence of different non-metals can result in different fractionation patterns, and that uniqueness offers the opportunity to gain insight into the evolution of planetary bodies.

1. Introduction

The separation of metal from silicate occurred during the early evolution of numerous planetary bodies in our solar system (e.g., Kleine et al., 2002; Schoenberg et al., 2002; Yin et al., 2002). The evolution of that separated metal continues today, as the central metallic cores of planets, like Earth, solidify (e.g., Jeanloz, 1990; Labrosse et al., 2001). The composition of the metal during these planetary processes affects how elements partition between the metallic core and the silicate mantle or between the solid inner core and the liquid outer core. Previous work has demonstrated that the presence of a "light" element in the metal, like S, P, or C, can especially influence the elemental partitioning behavior (Willis and Goldstein, 1982; Jones and Drake, 1983; Jones and Malvin, 1990). The effects of S, and to a lesser extent the effects of P, on solid metal/liquid metal partitioning have been examined by previous studies (compiled in Chabot et al., 2003; Chabot and Jones, 2003).

Carbon has been suggested as a potentially important light element in the central metallic cores of larger-than-asteroid-sized planetary bodies (Wood, 1993). Models of core formation in the Earth have included a variable to account for effects due to the presence of C in the segregating metal (Righter and Drake, 1999). Cohenite ($(Fe,Ni)_3C$) and graphite have been found in differentiated meteorites (e.g., Buchwald, 1975; Goodrich, 1992), which is evidence that C was present during the evolution of these materials. It is thus of interest to understand the influence of C on elemental partitioning behavior.

* Corresponding author. Fax: +1 240 228 8939.
E-mail address: Nancy.Chabot@jhuapl.edu (N.L. Chabot).
[1] Present address: Department of Geology, University of Maryland, College Park, MD 20742, USA.

0016-7037/$ - see front matter © 2005 Elsevier Inc. All rights reserved.
doi:10.1016/j.gca.2005.11.011

Despite the planetary applications, experimental data that have demonstrated the influence of C on elemental partitioning behavior are limited. Three experimental studies have examined the effect of C on partitioning between solid metal and liquid metal in the Fe–Ni–C system at 1 atm. Willis and Goldstein (1982) examined the behavior of six elements, though some elements such as Au, Cr, and Cu, were only present in one experiment each. Jones and Goodrich (1989) discussed the influence of C on the partitioning of Au, Ge, Ir, and Ni, elements also examined by Willis and Goldstein (1982), while Lauer and Jones (1999) systematically determined the partitioning behavior of Ni and W in the Fe–Ni–C system. Experimental data on the influence of C in metal/silicate systems are also largely lacking. Jana and Walker (1997) compared metal/silicate experiments conducted in C-free and graphite-saturated conditions for five elements, but no experiments were conducted at intermediate C contents. Chabot and Agee (2003) systematically determined the effect of C on the metal/silicate partitioning of V, Cr, and Mn, and Chabot et al. (2005) conducted similar experiments for Ni and Co.

The main purpose of this study was to improve our understanding of how trace elements partition between liquid and solid in the Fe–Ni–C system at 1 atm. Experimental charges were doped with 16 trace elements, and the low detection limits of laser ablation ICP-MS microanalysis techniques (Campbell and Humayun, 1999a,b; Campbell et al., 2002) were utilized to measure the partition coefficients. This is the first study to examine the effect of C on the partitioning behavior for many of these trace elements. After presenting the experimental data, the implications of these data for parameterization methods are discussed, as are some applications of the C-bearing data to the evolution of planetary bodies.

2. Experimental and analytical methods

Experimental and analytical methods were similar to those described in Chabot et al. (2003), where solid/liquid experiments were conducted in the Fe–Ni–S system. Starting compositions were mixed from commercially purchased powders of Fe, Ni, and graphite, with trace elements added at a concentration of approximately 100–400 ppm each from powders of As, Au, Co, Cr_2O_3, Cu, Ga, Ge, Ir, Os, Pd, Pt, Ru, Re, Sb, Sn, and H_2WO_4. About 200 mg of the starting mixture was loaded into a dense alumina crucible, which was in turn placed in a silica tube and evacuated. During the evacuation procedure, the crucible was heated with a torch until it glowed red to drive off any volatiles that could present a problem when the evacuated tube was later heated in the furnace. We believe during this process, some amount of C was lost as CO and CO_2, since it was routinely necessary to begin with more C in the starting mixture than would be predicted from the Fe–C phase diagram (Okamoto, 1990). However, experience has shown that this heating step is crucial to prevent the tubes from later expanding and fracturing at run conditions. The evacuated silica tube was then sealed and inserted into a Deltech vertical furnace at NASA Johnson Space Center. Each experimental charge was initially held at a temperature that was 30–150 °C higher than the final run temperature for 2 h, except for the highest temperature run at 1480 °C for which such a procedure was not possible. This step served to raise the temperature above the Fe–Ni–C liquidus, completely melting and homogenizing the starting material. The temperature was then lowered to the final run temperature, where the experiment was allowed to fully equilibrate. Final run temperatures ranged from 1200 to 1480 °C, with the temperature being monitored continuously with Pt_6Rh_{94}–$Pt_{30}Rh_{70}$ (type B) thermocouples calibrated against the melting point of Au. The run temperature did not drift by more than 3 °C during even the longest duration experiments. Run durations, which varied inversely with the run temperatures, ranged from 12 to 144 h and were based on obtaining equilibrium in previous solid metal/liquid metal experimental studies (e.g., Jones and Drake, 1983; Chabot et al., 2003). Run durations and temperatures are given in Table 1. Upon removal from the furnace, runs were quenched by immediately submersing the silica tubes in cold water.

Fig. 1 shows a back-scattered electron (BSE) image of a typical run product. The solid metal and liquid metal form two well separated phases. The solid metal is homogenous, but the liquid metal, which was a single phase at the run temperature, quenches to a dendritic texture of Fe–Ni-rich dendrites surrounded by C-rich material. At lower C contents (higher temperatures), the compositional difference between the solid and liquid metal phases is decreased, occasionally making it difficult to distinguish the two phases. In these cases, runs (#C4 and #C7) were etched for about 10 min with Nital to determine and photograph the locations of the solid and liquid metal. These two runs were then ground down again, to remove all trace of the etching process, and re-polished.

Experimental run products were first analyzed for the major elements Fe and Ni using an electron microprobe, either the University of Arizona Cameca SX-50 or the Smithsonian Institution National Museum of Natural History JEOL JXA 8900R. The measured Fe and Ni compositions of each experiment are given in Table 1. Beam conditions of 15–20 kV and 20 nA, with a counting time of 20 s on peak, were used. A defocused beam of 50 μm was used for all analyses and corresponding calibrations. To determine the bulk Fe and Ni concentrations of the quenched metallic liquid, which was multi-phased, 20–40 analysis points were averaged, while the homogeneous solid metal composition was determined from averages of 10–25 analysis points. Errors were calculated as twice the standard error of the mean of the multiple microprobe measurements. Prior to analysis with the 50 μm defocused beam, a point beam was used to examine the solid metal for Fe and Ni compositional gradients; no compositional gradients were observed, as expected for an equilibrium run product. As will be discussed in the next section, our

Table 1
Compositions of solid and liquid metal phases

Run #	C16	C6	C15	C9	C2	C13	C3	C12	C4	C7
Temperature (°C)	1200	1250	1280	1310	1350	1360	1390	1400	1450	1480
Duration (h)	144	61	77	35	38	33	43	12	20	12
Liquid metal										
Fe (wt%)	87.4 ± 0.2	85.4 ± 0.4	85.8 ± 0.2	87.4 ± 0.2	85.9 ± 0.2	89.3 ± 0.2	86.4 ± 0.2	88.6 ± 0.2	87.1 ± 0.4	87.8 ± 0.4
Ni (wt%)	7.5 ± 0.4	8.2 ± 0.3	10.3 ± 0.5	8.9 ± 0.2	9.1 ± 0.2	8.6 ± 0.2	9.5 ± 0.2	9.5 ± 0.2	9.2 ± 0.1	9.5 ± 0.1
C (wt%)	3.8	3.6	3.3	3.0	2.5	2.4	2.1	2.0	1.4	1.0
As (ppm)	266 ± 37	205 ± 7	136 ± 10	167 ± 12	205 ± 19	130 ± 12	143 ± 20	184 ± 37	113 ± 15	107 ± 12
Au (ppm)	142 ± 17	168 ± 7	170 ± 4	185 ± 2	195 ± 5	182 ± 4	184 ± 6	205 ± 4	173 ± 4	163 ± 7
Co (ppm)	286 ± 10	150 ± 5	290 ± 8	180 ± 4	160 ± 6	250 ± 4	161 ± 6	238 ± 12	215 ± 2	226 ± 4
Cr (ppm)	69 ± 10	65 ± 4	43 ± 2	59 ± 2	57 ± 6	45 ± 2	52 ± 5	46 ± 4	44 ± 2	42 ± 2
Cu (ppm)	267 ± 6	232 ± 25	308 ± 14	157 ± 7	123 ± 7	185 ± 8	130 ± 8	251 ± 27	264 ± 7	217 ± 28
Ga (ppm)	33 ± 4		59 ± 2			83 ± 2		91 ± 12		
Ge (ppm)	109 ± 10	129 ± 6	125 ± 8	147 ± 4	134 ± 5	129 ± 4	131 ± 6	124 ± 8	138 ± 5	134 ± 4
Ir (ppm)	21 ± 8	45 ± 8	77 ± 6	63 ± 8	59 ± 5	118 ± 10	78 ± 5	81 ± 12	129 ± 6	153 ± 10
Os (ppm)	30 ± 8	41 ± 6	64 ± 6	51 ± 6	43 ± 3	96 ± 8	54 ± 5	56 ± 10	89 ± 5	105 ± 5
Pd (ppm)	101 ± 15	131 ± 7	139 ± 8	151 ± 7	146 ± 4	152 ± 4	156 ± 5	141 ± 6	152 ± 5	156 ± 12
Pt (ppm)	23 ± 8	43 ± 7	70 ± 6	59 ± 7	59 ± 4	95 ± 6	74 ± 3	77 ± 10	100 ± 4	116 ± 7
Re (ppm)	92 ± 8	89 ± 9	94 ± 8	91 ± 8	75 ± 5	108 ± 6	74 ± 5	86 ± 16	101 ± 5	114 ± 8
Ru (ppm)	82 ± 12	103 ± 10	107 ± 8	107 ± 11	95 ± 5	128 ± 8	106 ± 6	111 ± 16	139 ± 6	156 ± 5
Sb (ppm)	302 ± 42	301 ± 18	211 ± 10	268 ± 9	268 ± 18	137 ± 12	196 ± 32	274 ± 73	200 ± 22	201 ± 10
Sn (ppm)	525 ± 69	289 ± 12	196 ± 10	431 ± 24	298 ± 26	255 ± 20	207 ± 27	234 ± 56	297 ± 39	287 ± 21
W (ppm)	288 ± 56	204 ± 29	126 ± 12	157 ± 10	152 ± 14	115 ± 14	114 ± 19	132 ± 37	106 ± 4	105 ± 5
Solid metal										
Fe (wt%)	86.9 ± 0.2	87.1 ± 0.4	85.6 ± 0.1	87.9 ± 0.3	87.4 ± 0.2	89.4 ± 0.2	87.9 ± 0.3	89.3 ± 0.3	89.5 ± 0.2	89.7 ± 0.2
Ni (wt%)	10.6 ± 0.1	10.4 ± 0.1	12.7 ± 0.1	10.4 ± 0.1	10.2 ± 0.1	9.0 ± 0.1	10.0 ± 0.1	9.8 ± 0.1	9.2 ± 0.1	9.1 ± 0.1
C (wt%)	1.8	1.6	1.4	1.2	1.0	0.9	0.8	0.7	0.4	0.3
As (ppm)	107 ± 2	84 ± 3	51 ± 2	66 ± 5	78 ± 17	42 ± 2	41 ± 2	57 ± 18	32 ± 1	31 ± 2
Au (ppm)	244 ± 6	195 ± 7	163 ± 8	166 ± 4	154 ± 8	125 ± 2	111 ± 4	114 ± 14	86 ± 2	75 ± 2
Co (ppm)	339 ± 4	173 ± 5	315 ± 8	191 ± 3	166 ± 7	266 ± 4	163 ± 6	246 ± 4	215 ± 6	229 ± 9
Cr (ppm)	31 ± 2	35 ± 1	25 ± 2	37 ± 1	37 ± 5	31 ± 2	35 ± 1	31 ± 4	35 ± 2	35 ± 2
Cu (ppm)	419 ± 14	276 ± 25	382 ± 8	186 ± 7	141 ± 8	219 ± 14	147 ± 8	231 ± 14	245 ± 9	158 ± 11
Ga (ppm)	98 ± 8		108 ± 4			118 ± 6		98 ± 6		
Ge (ppm)	179 ± 6	163 ± 9	138 ± 8	149 ± 6	118 ± 5	118 ± 8	95 ± 6	99 ± 4	104 ± 5	101 ± 4
Ir (ppm)	286 ± 69	204 ± 16	297 ± 18	197 ± 15	151 ± 19	365 ± 28	166 ± 10	204 ± 16	288 ± 8	294 ± 20
Os (ppm)	203 ± 18	138 ± 13	197 ± 14	134 ± 8	103 ± 13	276 ± 24	115 ± 7	141 ± 16	211 ± 11	240 ± 27
Pd (ppm)	213 ± 4	191 ± 7	171 ± 12	168 ± 4	137 ± 6	141 ± 8	117 ± 5	113 ± 4	107 ± 4	103 ± 6
Pt (ppm)	197 ± 35	144 ± 9	191 ± 14	134 ± 8	107 ± 11	199 ± 16	112 ± 7	129 ± 6	149 ± 6	147 ± 11
Re (ppm)	146 ± 12	127 ± 12	137 ± 10	131 ± 7	104 ± 10	187 ± 18	107 ± 7	146 ± 14	198 ± 11	232 ± 29
Ru (ppm)	193 ± 12	180 ± 15	184 ± 12	164 ± 9	134 ± 10	221 ± 20	142 ± 11	167 ± 12	216 ± 7	226 ± 20
Sb (ppm)	166 ± 6	133 ± 11	86 ± 4	106 ± 8	104 ± 30	43 ± 2	50 ± 2	77 ± 36	40 ± 2	36 ± 2
Sn (ppm)	291 ± 8	131 ± 11	82 ± 4	170 ± 16	118 ± 36	79 ± 4	54 ± 4	65 ± 30	59 ± 3	51 ± 2
W (ppm)	69 ± 4	76 ± 15	49 ± 2	74 ± 7	72 ± 11	62 ± 6	60 ± 4	86 ± 6	97 ± 5	121 ± 15

Measurements of Fe and Ni were made using the electron microprobe. Carbon contents were estimated based on the Fe–C phase diagram and run temperature. All other elements were analyzed by laser ablation ICP-MS. Errors are $\pm 2\sigma$.

partitioning results are in good agreement with the limited previous data, further supporting the attainment of equilibrium in and reproducibility of our experiments. A simple mass balance using the starting composition would require knowledge about the relative fractions of solid and liquid present in each charge; however, experience has shown that different slices through the same charge can expose significantly different amounts of solid and liquid, so this quantity cannot be accurately predicted without multiple prepared sections.

Directly analyzing C with the electron microprobe is complicated by the deposition of C on the sample by the beam, resulting in increased values for the "measured" C contents with time spent in the microprobe (Wood, 1993; Jana and Walker, 1997). The C background level also has to be established, which is likely to vary between different microprobes. Additionally, reliable and homogeneous C standards are required, and our inspection of multiple samples of NIST issued steels revealed them to be heterogeneous on scales up to 100 μm. Paying careful attention to these complications, Wood (1993) was still only able to reproduce C measurements to within 0.25 wt% using the electron microprobe. Because of these complications, we have chosen, like previous experimental studies (Willis and Goldstein, 1982; Jones and Goodrich, 1989; Lauer and Jones, 1999), to estimate the C contents of the solid metal and liquid metal using the Fe–C phase diagram (Okamoto, 1990). The effect of ~10 wt% Ni in the runs on the phase diagram was treated as negligible, and inspection of the Fe–Ni–C phase diagram (Raynor and Rivlin, 1988) indicates that the addition of

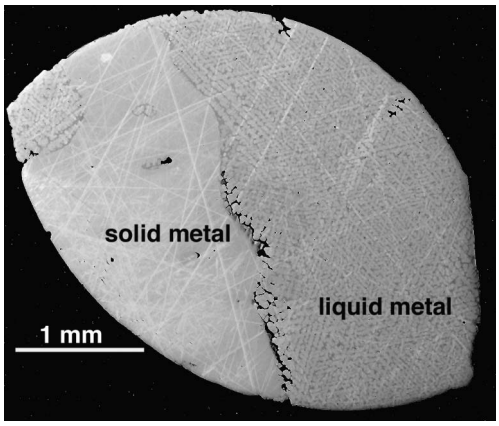

Fig. 1. A back-scattered electron (BSE) image of run #C2, conducted at 1350 °C, is shown. The liquid metal contains about 2.5 wt% C and quenched to a dendritic texture. The solid metal is homogenous, showing no signs of gradients.

~10 wt% Ni at a given temperature decreases the estimated C content by a few tenths of a wt%. Thus, we estimate the uncertainty in our C estimates at ~0.5 wt%. The estimated C contents were not used to correct the measurements of Fe and Ni by the microprobe. However, as discussed below, this does not affect the reported partitioning results, which were determined by laser ablation ICP-MS microanalysis techniques. Additionally, in each experimental run product, Ni concentrations were measured using both electron microprobe and laser ablation ICP-MS techniques; the measured values agreed to within 10% of each other, giving additional confidence in both analytical methods.

The concentrations of the trace elements were analyzed by laser ablation ICP-MS microanalysis at the University of Chicago. For each run product, the locations to be analyzed were selected from a BSE image of the sample, acquired with either the University of Arizona Cameca SX-50 or the Case Western Reserve University ARL-SEMQ electron microprobe, the University of Chicago JEOL 5800LV scanning electron microscope, or from a photograph of the sample. Laser ablation ICP-MS analyses were performed using a CETAC LSX-200 laser ablation peripheral with a magnetic sector ICP mass spectrometer, the Finnigan Element™, using techniques similar to those described by Campbell and Humayun (1999a), Campbell et al. (2002), and Chabot et al. (2003). Measurements were made by ablating line scans that were 50 μm wide, 300 μm long, and ~13 μm deep, produced by firing the laser at 10 Hz while scanning the sample at 20 μm/s for 15 s. This line scan method served to minimize any effects from the dendritic quench texture of the metallic liquid. During the analyses, the mass spectrometer was swept repeatedly over the mass range of interest, once per 0.8 s, and counts were accumulated at selected masses. To maximize signal to noise ratios and to avoid overlap with isotopes of neighboring elements or background sources, the following isotopes were measured during analysis: ^{53}Cr, ^{57}Fe, ^{59}Co, ^{60}Ni, ^{63}Cu, ^{69}Ga, ^{74}Ge, ^{75}As, ^{101}Ru, ^{105}Pd, ^{118}Sn, ^{121}Sb, ^{182}W, ^{185}Re, ^{192}Os, ^{193}Ir, ^{195}Pt, and ^{197}Au. Background subtractions were performed using the average of three blank measurements that were run either immediately before or after each set of analyses. Instrumental sensitivity factors for each isotope relative to ^{57}Fe were determined by measuring the signal intensity from the known standards of Hoba and NIST SRM 1263a (Campbell et al., 2002). The corrected intensities were normalized to 100%, taking into account the estimated amount of C expected in both the solid metal and liquid metal phases according to the Fe–C phase diagram (Okamoto, 1990). Reported errors in Table 1 were calculated as twice the standard error of the mean of five replicate analyses of each phase.

3. Partitioning results

The solid metal/liquid metal weight ratio partition coefficient (D) for an element E is calculated as:

$$D(E) = \frac{C_E^{\text{solid metal}}}{C_E^{\text{liquid metal}}}, \quad (1)$$

where C_E is the concentration (in wt%) for the element E in either the solid metal or liquid metal.

The partition coefficients determined from the experiments are tabulated in Table 2. In the experiments, the partition coefficients for the majority of the trace elements increased as the C content of the metallic liquid increased; Fig. 2 shows the partitioning results for the 14 elements that exhibited such behavior in the experiments. As the C content of the metallic liquid increased from the C-free system to near the Fe–C eutectic composition of about 4.3 wt% C (Okamoto, 1990), the solid/liquid partition coefficients of some elements, such as Ir and Pt, increased by nearly an order of magnitude. For other elements, such as As, Co, Ni, and Ru, the effect of C is much less pronounced, resulting in less than a factor of two variation.

Previous solid/liquid partitioning studies in the Fe–Ni–C system were carried out by Willis and Goldstein (1982), Jones and Goodrich (1989), and Lauer and Jones (1999). The results of these previous experimental studies (the latter two of which were reported in abstract form only) are tabulated in the Appendix A. Carbon contents were not measured in these previous studies. For consistency, the C contents of the previous studies were determined from the run temperature of each experiment and the Fe–C phase diagram (Okamoto, 1990), the same method used to determine the C contents of our run products. As shown on Fig. 2, for Au, Cu, Ge, Ir, and Ni, the partitioning results from our experiments are in good overall agreement with the limited previous studies. For the other nine elements shown in Fig. 2, our data are the first in the Fe–Ni–C system.

Out of the 17 elements examined, three were observed to have C-loving partitioning behaviors, with partition coefficients that decreased as the C content of the metallic liquid increased. We have chosen to adopt the new term of *anthracophile*, derived from Greek roots (*anthraco-*, coal or carbon, and *philos*, loving), to describe an element's behavior that is

Table 2
Partitioning results for experiments

Run #	C16	C6	C15	C9	C2	C13	C3	C12	C4	C7
Temperature (°C)	1200	1250	1280	1310	1350	1360	1390	1400	1450	1480
wt% C (liq.)	3.8	3.6	3.3	3.0	2.5	2.4	2.1	2.0	1.4	1.0
D(Ni)	1.42 ± 0.08	1.27 ± 0.07	1.24 ± 0.06	1.17 ± 0.05	1.12 ± 0.04	1.05 ± 0.03	1.06 ± 0.03	1.03 ± 0.03	0.99 ± 0.03	0.96 ± 0.05
D(As)	0.40 ± 0.06	0.41 ± 0.02	0.38 ± 0.03	0.40 ± 0.04	0.38 ± 0.09	0.32 ± 0.03	0.29 ± 0.04	0.31 ± 0.12	0.28 ± 0.04	0.29 ± 0.04
D(Au)	1.7 ± 0.2	1.16 ± 0.06	0.96 ± 0.05	0.90 ± 0.02	0.79 ± 0.04	0.69 ± 0.02	0.60 ± 0.03	0.56 ± 0.07	0.50 ± 0.02	0.46 ± 0.02
D(Co)	1.19 ± 0.04	1.15 ± 0.05	1.08 ± 0.04	1.06 ± 0.03	1.04 ± 0.06	1.06 ± 0.02	1.01 ± 0.05	1.03 ± 0.05	1.00 ± 0.03	1.01 ± 0.04
D(Cr)	0.45 ± 0.07	0.54 ± 0.03	0.58 ± 0.05	0.63 ± 0.03	0.65 ± 0.11	0.68 ± 0.05	0.67 ± 0.06	0.67 ± 0.1	0.80 ± 0.05	0.83 ± 0.05
D(Cu)	1.57 ± 0.06	1.2 ± 0.2	1.24 ± 0.06	1.19 ± 0.07	1.15 ± 0.09	1.19 ± 0.09	1.13 ± 0.09	0.92 ± 0.12	0.93 ± 0.04	0.73 ± 0.10
D(Ga)	3.0 ± 0.4		1.82 ± 0.09			1.42 ± 0.08		1.1 ± 0.2		
D(Ge)	1.6 ± 0.2	1.26 ± 0.09	1.11 ± 0.09	1.01 ± 0.05	0.88 ± 0.05	0.92 ± 0.07	0.73 ± 0.06	0.80 ± 0.06	0.75 ± 0.05	0.75 ± 0.04
D(Ir)	14 ± 6	4.6 ± 1.0	3.8 ± 0.4	3.1 ± 0.5	2.6 ± 0.4	3.1 ± 0.4	2.1 ± 0.2	2.5 ± 0.4	2.2 ± 0.1	1.9 ± 0.2
D(Os)	7 ± 2	3.4 ± 0.6	3.1 ± 0.4	2.6 ± 0.4	2.4 ± 0.4	2.9 ± 0.3	2.1 ± 0.2	2.5 ± 0.5	2.4 ± 0.2	2.3 ± 0.3
D(Pd)	2.1 ± 0.3	1.5 ± 0.1	1.2 ± 0.1	1.11 ± 0.06	0.94 ± 0.05	0.92 ± 0.06	0.75 ± 0.04	0.80 ± 0.04	0.70 ± 0.03	0.66 ± 0.06
D(Pt)	9 ± 3	3.4 ± 0.6	2.8 ± 0.3	2.3 ± 0.3	1.8 ± 0.2	2.1 ± 0.2	1.5 ± 0.1	1.7 ± 0.2	1.5 ± 0.1	1.3 ± 0.1
D(Re)	1.6 ± 0.2	1.4 ± 0.2	1.5 ± 0.2	1.5 ± 0.2	1.4 ± 0.2	1.7 ± 0.2	1.5 ± 0.1	1.7 ± 0.4	2.0 ± 0.1	2.0 ± 0.3
D(Ru)	2.4 ± 0.4	1.8 ± 0.2	1.7 ± 0.2	1.5 ± 0.2	1.4 ± 0.1	1.7 ± 0.2	1.3 ± 0.1	1.5 ± 0.2	1.6 ± 0.1	1.4 ± 0.1
D(Sb)	0.55 ± 0.08	0.44 ± 0.04	0.41 ± 0.03	0.40 ± 0.03	0.39 ± 0.11	0.31 ± 0.03	0.26 ± 0.04	0.28 ± 0.15	0.20 ± 0.02	0.18 ± 0.01
D(Sn)	0.55 ± 0.07	0.45 ± 0.04	0.42 ± 0.03	0.39 ± 0.04	0.4 ± 0.1	0.31 ± 0.03	0.26 ± 0.04	0.28 ± 0.14	0.20 ± 0.03	0.18 ± 0.01
D(W)	0.24 ± 0.05	0.37 ± 0.09	0.39 ± 0.04	0.47 ± 0.05	0.47 ± 0.09	0.54 ± 0.08	0.52 ± 0.09	0.7 ± 0.2	0.91 ± 0.06	1.2 ± 0.2

Errors are ±2σ. Carbon contents were estimated based on the Fe–C phase diagram and run temperature. *D*(Ni) was calculated using electron microprobe analyses, while other partition coefficients were determined using laser ablation ICP-MS data.

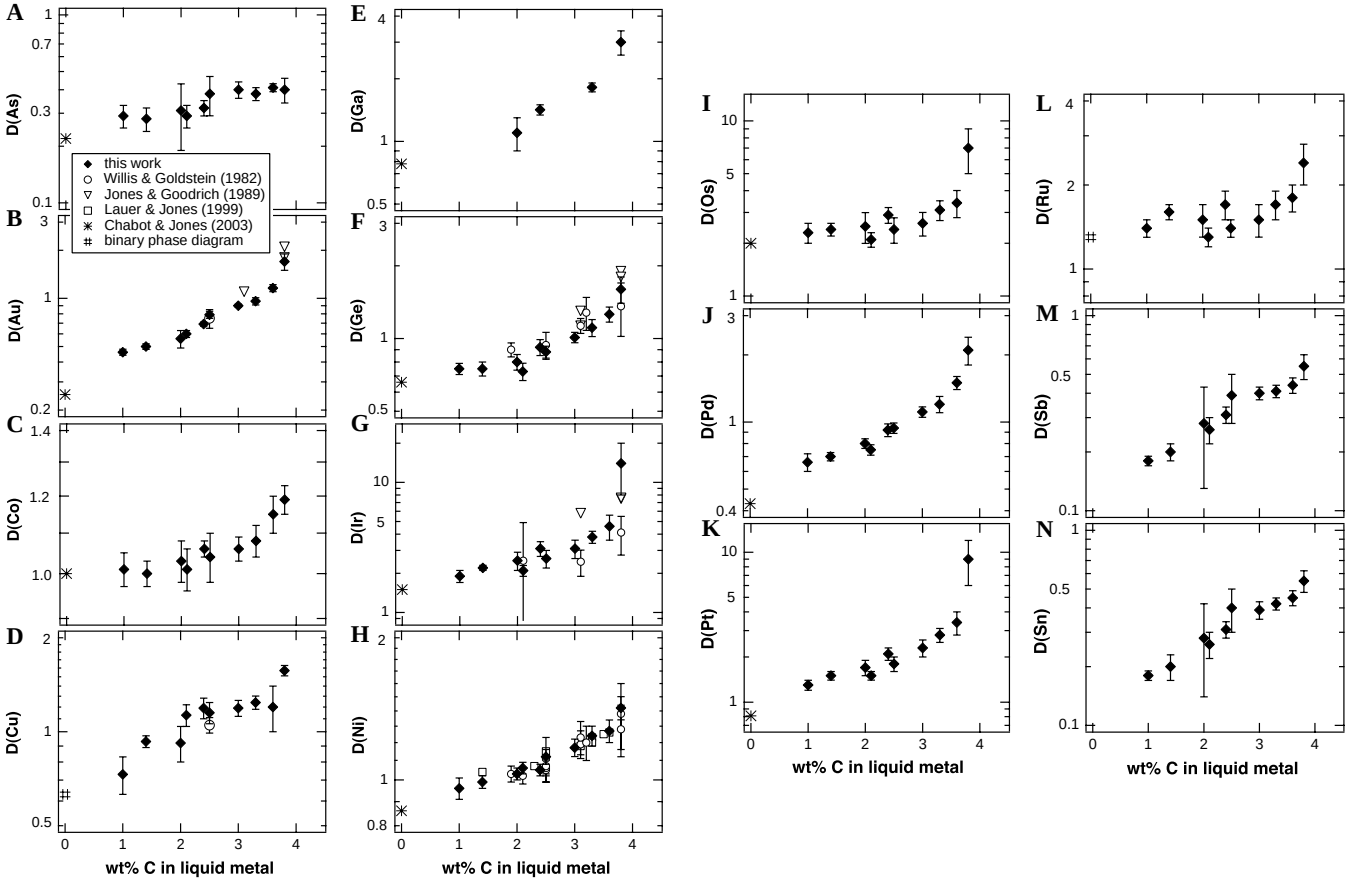

Fig. 2. The solid/liquid partition coefficients (*D*) for (A) As, (B) Au, (C) Co, (D) Cu, (E) Ga, (F) Ge, (G) Ir, (H) Ni, (I) Os, (J) Pd, (K) Pt, (L) Ru, (M) Sb, and (N) Sn are plotted as a function of the C content of the metallic liquid. The partition coefficients for all of these elements increase as the C content of the metallic liquid increases. Our experimental results are in general agreement with the limited previous experimental studies (Willis and Goldstein, 1982; Jones and Goodrich, 1989; Lauer and Jones, 1999) and with partitioning behaviors in the non-metal-free system as determined by the parameterizations of Chabot and Jones (2003) and from the binary phase diagrams (Elliott, 1965; Moffatt, 1986). Error bars are ±2σ.

C-loving. Precedent for this nomenclature stems from the use of Greek roots to describe, for example, rock-loving (lithophile: *lithos*, rock) and iron-loving (siderophile: *sidero*-, iron) elemental behavior. The partitioning data of the anthracophile elements Cr, Re, and W are plotted in Fig. 3. Our experimental results are in good agreement with the one previous determination of D(Cr) by Willis and Goldstein (1982) and the systematic study of D(W) by Lauer and Jones (1999). Our study of Re partitioning is the first to examine the influence of C. The elements W and Cr are known to form carbides; the compound WC is known for its extreme hardness, and multiple binary Cr-bearing carbides are known to be stable (Greenwood and Earnshaw, 1984). Thus, the formation of stable carbides by an element may predict anthracophile tendencies.

Also plotted on Figs. 2 and 3 are the elemental partition coefficients as calculated by Chabot and Jones (2003) for a metallic liquid containing no C, S, or other non-metal. For Cu and Ru, which were not parameterized by Chabot and Jones (2003), partitioning values in the C-free system were estimated from binary phase diagrams with solid Fe in the face-centered cubic (fcc, γ) phase (Elliott, 1965; Moffatt, 1986). For Cr, Sb, and Sn, the binary phase diagrams provided information for partitioning involving solid metal with a body-centered cubic (bcc, α) structure, and consequently such phase diagram information was not appropriate for comparison to our experimental data. The partition coefficients taken from both the Chabot and Jones (2003) parameterizations and the binary phase diagrams with γFe stable are generally consistent with the trends from our C-bearing data, as shown in Figs. 2 and 3.

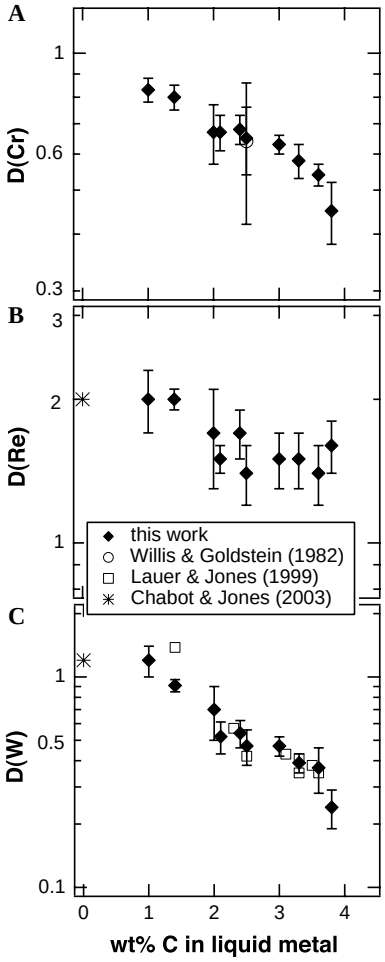

Fig. 3. The solid/liquid partition coefficients (D) for (A) Cr, (B) Re, and (C) W are shown as a function of the C content of the metallic liquid. In contrast to the elements plotted in Fig. 2, these three elements exhibit anthracophile (C-loving) behavior, with the elements partitioning more strongly into the metallic liquid as the C content of the metallic liquid increases. Our new experimental data are consistent with the previous W study of Lauer and Jones (1999), the one previous Cr-bearing experiment of Willis and Goldstein (1982), and the non-metal-free partition coefficients determined by the parameterizations of Chabot and Jones (2003). The error bars are ±2σ.

For all of the elements examined, a consistent partitioning trend was observed when elements within the same column of the periodic table were compared. Within a given column, the element with the larger atomic number exhibited a greater change in its partition coefficient as a function of the C content of the metallic liquid. A comparison of the three elements Ni, Pd, and Pt illustrates this trend, with D(Ni) only varying by a factor of ~1.5, D(Pd) by a larger factor of ~3, and D(Pt) by the largest factor of ~7. Similar comparisons can be drawn for the same column element pairs of As–Sb, Cu–Au, Co–Ir, Ge–Sn, and Ru–Os. The behavior of the same column anthracophile elements Cr and W is also consistent with this trend, with the higher atomic number element W showing a larger variation in its partition coefficient with the changing C content of the metallic liquid.

4. A comparison to parameterization predictions

The composition of the metallic liquid, specifically the concentration of any non-metal such as S, P, or C, can have a significant effect on the resulting solid metal/liquid metal partition coefficients (Willis and Goldstein, 1982; Jones and Drake, 1983). Jones and Malvin (1990) introduced an expression for parameterizing solid/liquid partition coefficients using the metallic liquid composition, not temperature, as the dominant influence on the partitioning behavior. In the Jones and Malvin (1990) method, the metallic liquid is approximated as being composed of non-metal-bearing "domains" and non-metal-free "domains". The calculation of the relative fraction of each type of "domain" depended on the assumed speciation of the non-metal in the metallic liquid (such as FeS, Fe_3P, Fe_3C, etc.). The effects of S, P, and C on partitioning behavior were parameterized as separate effects in the Jones and Malvin (1990) method, and partitioning in systems with multiple non-metals (such as the Fe–Ni–S–P system) was treated by calculating weighted averages of the behaviors in the end-member single non-metal systems.

Using the same general picture of the metallic liquid as being composed of domains, Chabot and Jones (2003) parameterized the partition coefficients of 13 siderophile elements. For elements whose partition coefficients increased as

the non-metal (C, S, or P) content of the metallic liquid increased, Chabot and Jones (2003) suggested that their partitioning behavior was dominantly influenced by the availability of non-metal-free domains (''Fe domains'') in the metallic liquid. That suggestion meant that the identity of the non-metal present in the metallic liquid was not the dominant variable but rather how that non-metal decreased the amount of ''Fe domains'' in the metallic liquid was the important parameter. In other words, in contrast to Jones and Malvin (1990); Chabot and Jones (2003) predicted that the partitioning behavior for an element that avoids non-metals was fundamentally the same in the Fe–Ni–S, Fe–Ni–P, Fe–Ni–C, and combinations of these systems if the partitioning behavior was examined as a function of the fraction of available ''Fe domains'' in the metallic liquid.

The experimental data for non-metal systems other than the Fe–Ni–S system were limited when Chabot and Jones (2003) developed their parameterization theory. With our new partitioning data in the Fe–Ni–C system, we can now test the Chabot and Jones (2003) prediction that their parameterizations, based on S-bearing experimental data, can also explain the partitioning behaviors observed in our C-bearing system. According to Chabot and Jones (2003), the partition coefficient is parameterized as:

$$\frac{1}{D} = \frac{(Fe\ domains)^{\beta}}{D_0}, \tag{2}$$

where D_0 is the partition coefficient in the non-metal-free Fe–Ni system and β is a constant specific to the element

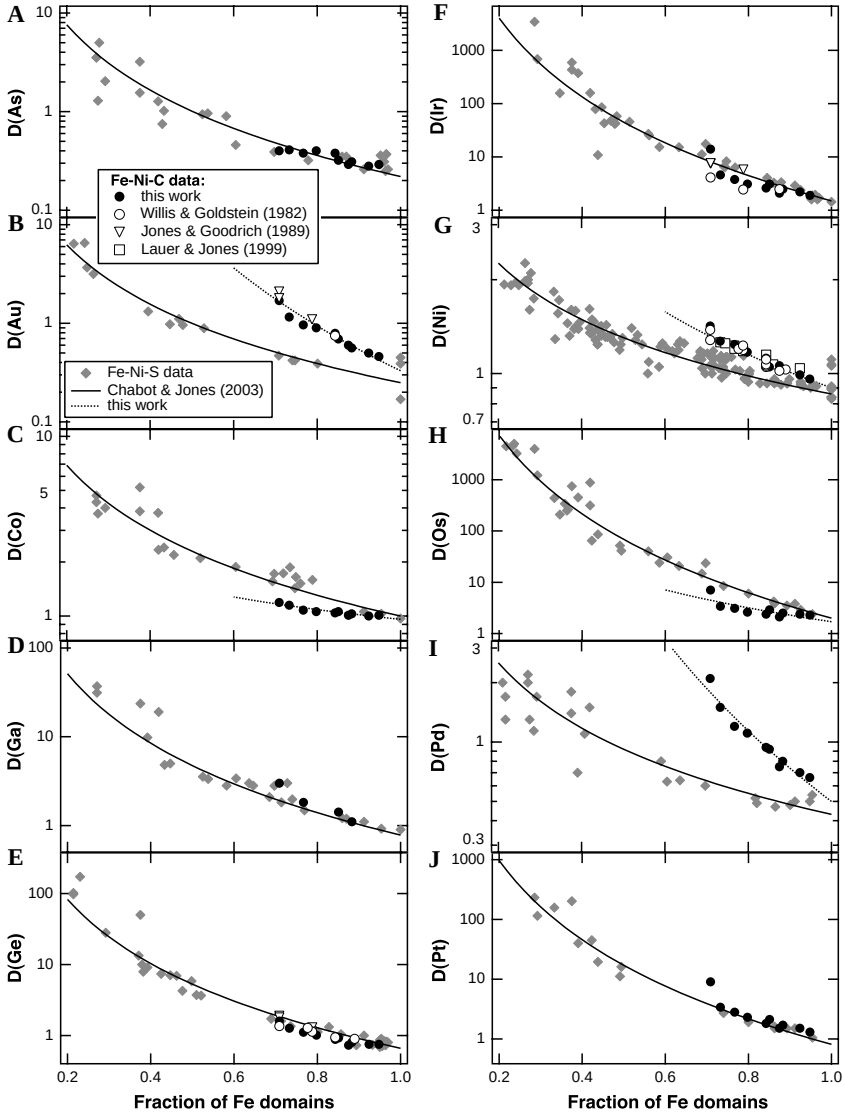

Fig. 4. Our results for partitioning in the Fe–Ni–C system are compared to previous experimental studies in the Fe–Ni–S system for the elements (A) As, (B) Au, (C) Co, (D) Ga, (E) Ge, (F) Ir, (G) Ni, (H) Os, (I) Pd, and (J) Pt. All experiments are plotted as a function of the *Fe domains* in the metallic liquid, with an assumed speciation of either Fe_3C or FeS. The parameterized fits of Chabot and Jones (2003) to the S-bearing data are also shown. For As, Ga, Ge, Ir, and Pt, the partitioning behaviors in the C-bearing and S-bearing systems are generally similar when examined as a function of the *Fe domains*, as predicted by Chabot and Jones (2003). However, the Chabot and Jones (2003) parameterizations do not provide an adequate match to D(Au), D(Co), D(Ni), D(Os), and D(Pd) in the Fe–Ni–C system, requiring new parameterizations that are shown as dotted lines. Experimental S-bearing data are compiled in Chabot and Jones (2003).

being parameterized. Assuming a speciation of Fe_3C in the metallic liquid, *Fe domains* is calculated as:

$$Fe\ domains = \frac{(1 - 4X_C)}{(1 - 3X_C)}, \quad (3)$$

where X_C is the mole fraction of C in the metallic liquid. The quantity of *Fe domains* in Eq. (3) is a fraction, calculated as the number of non-metal-free domains divided by the total number of domains (non-metal-free + non-metal-bearing) in the metallic liquid.

Our experimental C-bearing data for 10 elements that exhibit both S and C avoidance in their partitioning behaviors are plotted in Fig. 4 as a function of the fraction of *Fe domains* in the metallic liquid, as calculated from Eq. (3). Experimental data from the Fe–Ni–S system (compiled in Chabot and Jones, 2003) are also plotted, as are the fitted parameterizations of Chabot and Jones (2003). For half of the elements in Fig. 4, specifically As, Ga, Ge, Ir, and Pt, the C-bearing and S-bearing data do seem to roughly fall within the scatter of each other when plotted as a function of the *Fe domains* in the metallic liquid; this is consistent with the prediction of the Chabot and Jones (2003) parameterization method. However, for the other five elements in Fig. 4, there are discrepancies between the C-bearing and S-bearing data sets that are much larger than the scatter in the experimental data. Furthermore, the partition coefficients of Au, Ni, and Pd are larger in the Fe–Ni–C system than in the Fe–Ni–S system but D(Co) and D(Os) show the opposite trend and are lower in the C-bearing experiments. Thus, the assumed speciation of C in the metallic liquid is not the cause of the discrepancies, since a different choice for the speciation would result in a similar shift to the partitioning data for all the elements, not a raising of some and a lowering of others.

It is interesting that the predicted Chabot and Jones (2003) behavior is consistent with the partition coefficients for some of the elements and inconsistent with others. A number of questions can be raised. What is different between the five elements that are fit and the five that are not? Is the success of the Chabot and Jones (2003) prediction for five of the elements a real success or is it a fortunate coincidence? One potentially important difference between solid/liquid partitioning in the Fe–Ni–S system and the Fe–Ni–C system is the composition of the solid metal. An assumption in the original parameterization of Jones and Malvin (1990), and also made by Chabot and Jones (2003), is that any effect from a change in the composition of the solid metal is negligible as compared to the effect from the changing composition of the liquid metal. In the S-bearing system, such an assumption is likely true, since the solubility of S in solid Fe–Ni metal is very low and the solid metal consequently remains essentially S-free while the metallic liquid will contain 31 wt% S at the Fe–S eutectic composition (Hansen, 1958). In contrast, in the C-bearing system, the solid metal can reach up to 2.1 wt% C at the Fe–C eutectic composition, where the liquid metal will only have 4.3 wt% C (Okamoto, 1990). Thus, it may not be valid to treat the variation in the composition of the solid metal as negligible when examining partitioning in the Fe–Ni–C system. If so, then the matches between experimental observations and the predictions of Chabot and Jones (2003) may have simply been fortuitous.

In seeking to identify differences between the five elements fit and the five not, we considered the possible influence of crystal structure. The two elements, Co and Os, that have lower partition coefficients in the C-bearing system than in the S-bearing system on Fig. 4 are the only 2 out of those 10 shown that have hexagonal close packed (hcp, ε) crystal structures as metals (Selle, 1974). The elements Au, Ni, and Pd exhibit face-centered cubic (fcc, γ) crystal structures (Selle, 1974) and, at a given fraction of *Fe domains*, have larger partition coefficients in the Fe–Ni–C system than in the Fe–Ni–S system; however, the elements Ir and Pt also form fcc metals (Selle, 1974) and their C-bearing partition coefficients are in general agreement with the Chabot and Jones (2003) parameterizations. As an interesting note, the only two elements studied that exhibit a body-centered cubic (bcc, α) crystal structure, Cr and W (Selle, 1974), both behaved as anthracophile elements in our experiments, as shown on Fig. 3. Despite these observations, the importance of the metallic crystal structure to the task of parameterizing solid/liquid partitioning behavior remains unclear.

For current parameterization purposes, in the Fe–Ni–C system, we recommend using the expressions given in Eqs. (2) and (3), values for which are given in Table 3. For those five elements whose partitioning behaviors in the Fe–Ni–C and Fe–Ni–S systems are described by the same fitted expression, we assume that the Chabot and Jones (2003) parameterizations can also be used to predict partitioning behaviors in the multiple non-metal Fe–Ni–S–C system. For the other five elements Au, Co, Ni, Os, and Pd, the fits shown on Fig. 4 and listed in Table 3 parameterize partitioning behavior in the Fe–Ni–C system only. However, in these cases, it is not clear how to predict the partitioning behavior of elements in the Fe–Ni–S–C system. Currently,

Table 3
Values for fitted parameterizations

For use in	D_0 (wt%)	β
Fe–Ni–C–S system		
As	0.22[a]	2.2[a]
Ga	0.78[a]	2.6[a]
Ge	0.66[a]	3.0[a]
Ir	1.5[a]	4.9[a]
Pt	0.81[a]	4.4[a]
Fe–Ni–C system only		
Au	0.33	4.7
Co	0.96	0.56
Ni	0.90	1.1
Os	1.7	2.8
Pd	0.50	3.7
Cu	0.78	1.9
Ru	1.2	1.3
Sb	0.17	3.5
Sn	0.17	3.5

[a] Values from the parameterizations of Chabot and Jones (2003). All others from this work.

a weighted average of the partitioning behaviors in the end member Fe–Ni–S and Fe–Ni–C systems, as was done by Jones and Malvin (1990), may be the best approximation. Table 3 also gives values for parameterizing D(Cu), D(Ru), D(Sb), and D(Sn) in the Fe–Ni–C system, elements which were not parameterized by Chabot and Jones (2003) in the Fe–Ni–S system. More work is needed to better understand elemental partitioning behaviors in metallic systems that contain multiple non-metals.

5. Planetary applications

5.1. Inner core–outer core fractionations

Recent ^{187}Re–^{187}Os and ^{190}Pt–^{186}Os studies have reported elevated Os isotopic ratios in mantle plume sources, leading to the suggestion that entrainment of outer core material in the mantle or isotopic exchange at the core–mantle boundary can account for this observed Os isotopic signature (Walker et al., 1995, 1997; Brandon et al., 1998, 1999, 2003; Meibom and Frei, 2002; Puchtel et al., 2005). To create elevated ^{187}Os/^{188}Os and ^{186}Os/^{188}Os ratios, the source region must contain some material that is enriched in Re and Pt relative to Os, with Pt/Re ~80. Both partitioning experiments (Walker, 2000; Chabot et al., 2003) and partitioning behaviors that have been inferred from iron meteorites (e.g., Walker et al., 1995) qualitatively suggest that crystallization of the Earth's solid inner core may increase the Re/Os and Pt/Os ratios in the liquid outer core while maintaining a high Pt/Re ratio. The results of W isotopic measurements to either disprove or support this suggestion are currently being debated (Schersten et al., 2004; Brandon and Walker, 2005).

Pressure is the single most important variable that limits applying our experiments directly to issues of inner core–outer core differentiation (>3 Mbar vs. 1 bar). However, high-pressure experimentally determined partition coefficients are not available for the pressure and temperature conditions of the inner core boundary. Thus, Walker et al. (1995) and subsequent workers (e.g., Brandon et al., 2003; Puchtel et al., 2005; Brandon and Walker, 2005) have used iron meteorites as natural analogs for elemental partitioning in models of core differentiation. While recognizing the evident limitations of pressure and temperature conditions, our experiments, and those compiled in Chabot et al. (2003), control at least one very important set of variables (C and S abundances) that are unconstrained in natural analogs. Fig. 5 shows the partitioning results for Pt, Re, and Os from our C-bearing experiments compared to previous S-bearing experiments (Chabot et al., 2003) and clearly illustrates that the effects from C are very different than the effects from S. These results show that different light elements can cause very different relative fractionations between Re–Os and Pt–Os, which would lead to different Os isotopic signatures. Thus, there is the potential that if the elevated Os isotopic ratios attributed to mantle plume sources are sampling the Earth's outer core, explaining this unique Os isotopic signature could give insight into the light element composition of the core.

To generate the Os isotopic signature that has been attributed to the Earth's outer core (Walker et al., 1995, 1997; Brandon et al., 1998, 1999, 2003; Meibom and Frei, 2002; Puchtel et al., 2005), the outer core needs to be enriched in both Pt and Re relative to Os. As shown in Fig. 5, low pressure, 1 atm experiments with only S or only C have not generated the needed fractionations of all three elements simultaneously. The presence of S can cause a significant enrichment of Pt relative to Os in the metallic liquid, but only a minor enrichment of Re relative to Os is generated with a S-bearing liquid. In contrast, a C-bearing metallic liquid can produce a larger enrichment of Re relative to Os, but, as the C content of the metallic liquid increases, the enrichment of Pt relative to Os decreases.

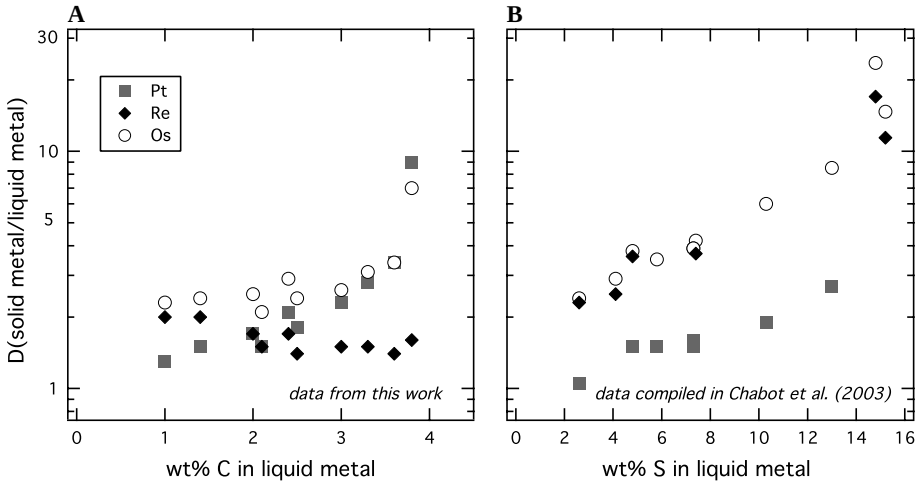

Fig. 5. The partitioning behavior of Pt, Re, and Os are compared in the (A) C-bearing and (B) S-bearing systems. The relative fractionations of these three elements are of particular interest because of the Re–Os and Pt–Os decay sequences. As shown, the relative fractionations of Pt, Re, and Os that would be caused by a C-bearing metallic liquid are quite different than those from a S-bearing liquid; thus, different non-metals in a metallic liquid will lead to different Os isotopic signatures. Experimental data from the Fe–Ni–S system are compiled in Chabot et al. (2003).

If C is present in the Earth's core, it is likely to be one of multiple light elements; carbon cannot account for the observed outer core density deficit of about 10% on its own (Wood, 1993; Hillgren et al., 2000). A review by Hillgren et al. (2000) suggests that there are likely multiple light elements in the Earth's outer core, with some possibilities including not only S and C, but also O and Si. There is clear motivation for additional experimental work involving other metallic compositions, compositions that contain multiple light elements, different solid Fe alloy crystal structures, and especially higher pressures.

5.2. Core formation

The metallic composition is one of the variables that will influence how elements partition during planetary core formation, when metal and silicate separate to form a central metallic core and a residual silicate mantle. During core formation, elements will partition between metal and silicate, where the metal may be a combination of solid and liquid metal, and the liquid metal phase is likely to have alloyed with S and/or C. Thus, the effects of C that we have determined in this work may have useful applications to planetary core formation.

Fig. 6 compares our solid metal/liquid metal data for D(Cr) to liquid silicate/liquid metal partitioning data for Cr from a study of Chabot and Agee (2003). Both studies show a similar effect of C on the partition coefficient of Cr. In our experiments, the changing composition of the liquid metal is the dominant influence on the partitioning behavior, and any effects from the solid metal appear to be small in comparison. In the Chabot and Agee (2003) experiments, the silicate composition, pressure, and temperature were all held constant and the metallic composition was varied, making it the dominant influence in the experiments. Thus, both sets of experiments were dominantly influenced by the C content of the metallic liquid, leading to similar partitioning results for Cr as shown in Fig. 6.

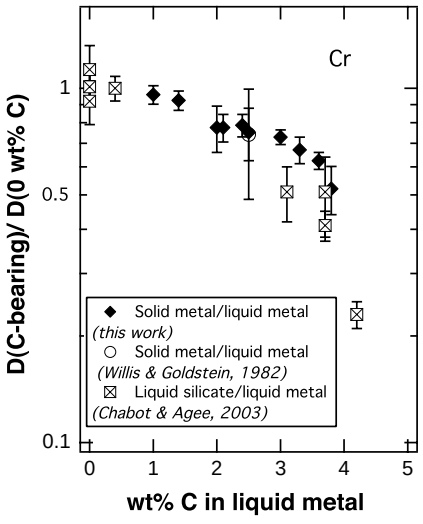

Fig. 6. The effect of C on the solid metal/liquid metal and liquid silicate/liquid metal partition coefficients for Cr are compared by plotting the C-bearing partition coefficients divided by the partitioning value in the C-free system. Though the absolute values of the partition coefficients in the two systems are different, the effect of C on the partition coefficients is similar. Error bars for both data sets are $\pm 2\sigma$.

The absolute values of the partition coefficients in the solid metal/liquid metal and liquid silicate/liquid metal systems are different, but the relative effect of C, the change in the partition coefficient from the C-free system to one with 3–4 wt% C, is the same. This similarity suggests that the effect of metallic composition as determined by solid metal/liquid metal experiments can potentially be applied to models of core formation. Righter et al. (1997) and subsequent core formation studies (Righter and Drake, 1999; Gessmann and Rubie, 2000; Li and Agee, 2001; Chabot et al., 2005) have developed equations to express metal/silicate partition coefficients as a function of the variables of pressure, temperature, oxygen fugacity, silicate composition, and metallic composition. Our results suggest the possibility that the effect of metallic composition can be determined from solid metal/liquid metal studies such as this one, parameterized as a function of the light element content of the metallic liquid (such as by Eqs. (2) and (3)), and potentially added on as an additional term to the larger metal/silicate expressions. The possibility of using solid metal/liquid metal data in core formation models is especially desirable because much more data are available for the effects of S (Chabot et al., 2003; Chabot and Jones, 2003) and C (this work) from experiments conducted in solid metal/liquid metal systems than in metal/silicate systems.

Metal/silicate partitioning data that have examined the effect of C are limited, but the few studies that have been completed in addition to the work of Chabot and Agee (2003) are also consistent with our solid metal/liquid metal results. For D(Co) and D(Ni), less than a factor of two change in the partition coefficients over the C range investigated was observed, as shown in Fig. 2; these small changes are within the scatter and error bars of the five liquid silicate/liquid metal experiments conducted by Chabot et al. (2005) that examined the effect of C on Ni and Co. Jana and Walker (1997) compared liquid silicate/liquid metal partitioning behavior in C-free and graphite-saturated conditions, finding that Ni and Co exhibited small increases in their silicate/metal partition coefficients, consistent with our solid metal/liquid metal results. Also consistent with our solid metal/liquid metal results, Jana and Walker (1997) found a larger increase in the silicate/metal partition coefficient for Ge than for Ni or Co and a decrease in the partition coefficient of the anthracophile element W, under graphite-saturated conditions. The comparisons are limited, but they further support the idea that solid metal/liquid metal partitioning data may be used to understand the effects of metallic composition during planetary core formation. Additionally, some metal/silicate partitioning experiments have been carried out in graphite-saturated conditions, without C-free control runs (e.g., Walter and Thibault, 1995; Li and Agee, 2001). Our results

may provide a way to correct these data for the effect of C, if the C content of the metallic melt in the experiments is known or can be estimated.

5.3. Meteorite parent bodies

The range of bulk C contents in iron meteorites varies, from the essentially C-free IVA and IVB iron meteorite groups to the IAB group with an estimated bulk C content of 0.2–2 wt% (Buchwald, 1975). In iron meteorites, some of the C is present in the mineral cohenite ($(Fe,Ni)_3C$) (Buchwald, 1975). Campbell and Humayun (1999b) measured the concentration of trace elements in cohenite from the IAB iron meteorite Odessa using laser ablation ICP-MS analysis techniques; McDonough et al. (1999) made similar measurements on the IAB iron Canyon Diablo. Fig. 7 compares the naturally occurring IAB partitioning behavior between cohenite and coexisting Fe–Ni kamacite to the partition coefficients measured in our experiment with 3.8 wt% C in the metallic liquid (#C16), the highest concentration of C in our experimental runs. It should be noted that the two reactions being compared on Fig. 7 are quite different. The solid/liquid partition coefficient is for an equilibrium reaction with a single C content of 3.8 wt% and thus a single temperature, while kamacite/cohenite partitioning in iron meteorites is a solid state reaction, occurring over a range of temperatures and also affected by diffusion and the meteorite's cooling rate. Despite these differences in the reactions, there is still a general correlation between the partition coefficients as determined by our experiment and the kamacite/cohenite partition coefficients measured in the two IAB irons, as seen on Fig. 7. In particular, the element W, which is observed to be anthracophile in our experiments, has kamacite/cohenite and solid metal/liquid metal partition coefficients that are both <1. Thus, the partitioning tendencies observed in our experiments are generally consistent with the natural partitioning tendencies that occurred in iron meteorite parent bodies.

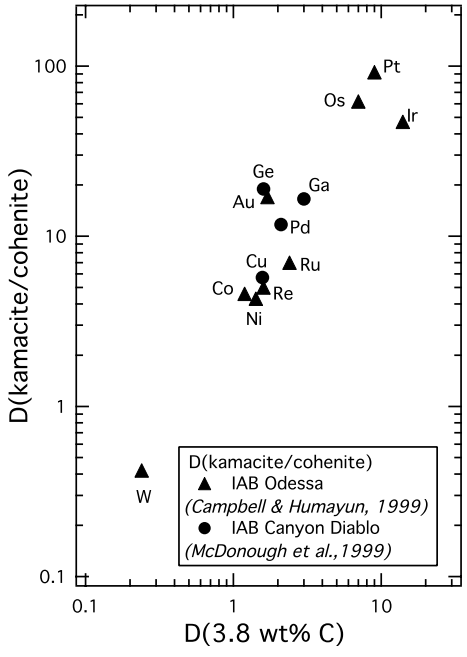

Fig. 7. The partitioning behavior between kamacite (Fe–Ni alloy) and cohenite ($(Fe,Ni)_3C$) as measured in the IAB iron meteorites Odessa (Campbell and Humayun, 1999b) and Canyon Diablo (McDonough et al., 1999) is compared to each element's experimentally determined solid metal/liquid metal partition coefficient with 3.8 wt% C in the metallic liquid. A general correlation is seen between the natural kamacite/cohenite partitioning tendencies and the partitioning tendencies as determined in our experiments.

Other meteorite groups also contain C and C-bearing phases. In ureilites, the second largest group of achondrites, C is most commonly observed as graphite (Goodrich, 1992). Recent studies have found a general correlation between siderophile element abundances in ureilites and solid/liquid partitioning behavior in the Fe–Ni–S system, suggesting partial melting with the loss of a S-rich metallic liquid occurred on the ureilite parent body (Humayun et al., 2005; Kallemeyn and Warren, 2005). If this melting process occurred in the presence of the graphite observed in ureilites, it could be expected that the metallic melt not only contained S but also contained C. As our experiments have shown, the solid/liquid partitioning behaviors expected from the presence of S as compared to the presence of C are not the same for all elements. In particular, the effects of S and C have opposite effects on the partition coefficients of W, Re, and Cu. D(W) and D(Re) both increase with increasing S content of the metallic liquid (e.g., Chabot and Jones, 2003) but decrease as the C content increases; D(Cu) decreases with increasing S content (Chabot et al., 2003) but increases as the C content increases. Because of the contrasting effects of S and C, the elements of W, Re, and Cu may consequently be useful in further constraining the origin of the siderophile element signature of ureilites. However, applying the experimental partitioning data to ureilites could involve partitioning in the Fe–Ni–S–C system, and, as has been discussed, more work is needed to understand partitioning behaviors in systems with multiple nonmetals. Additionally, if the history of ureilites did involve an Fe–Ni–S–C liquid, the possibility of encountering liquid immiscibility should also be considered (Raghavan, 1988).

6. Summary

In conclusion, we have examined the effect the presence of C in a metallic liquid has on the partitioning behavior of 17 elements, and for many of these elements, this study offers the first such data. The solid/liquid partition coefficients for the elements As, Au, Co, Cu, Ga, Ge, Ir, Ni, Os, Pd, Pt, Ru, Sb, and Sn increase as the C content of the metallic liquid increases. In contrast, Cr, Re, and W behave as anthracophile (C-loving) elements, and their partition coefficients decrease with increasing concentrations of C in the metallic liquid.

Previous parameterizations of solid/liquid partition coefficients can explain some but not all of our new experimental data. The presence of either S or C causes the solid/liquid

partition coefficients for Au, Co, Ni, Os, and Pd to increase, but the parameterizations of Chabot and Jones (2003) do not adequately express the effects of both S and C on these elements' partitioning behaviors. However, for the five elements As, Ga, Ge, Ir, and Pt, the Chabot and Jones (2003) expressions derived from S-bearing data provide good matches to the new C-bearing experimental results.

Extrapolating our experimental results to the solidification of the Earth's core suggests that the presence of C would lead to fractionations between Pt, Re, and Os that were different than fractionations caused by the presence of S. Additionally, we demonstrate that the effect of C on partitioning behavior, as determined from our solid metal/liquid metal data, can potentially be applied to metal/silicate systems and included in models of planetary core formation to predict trends in elemental fractionations. Our experimental data are also consistent with the composition of naturally occurring cohenite in iron meteorites and may be specifically useful for interpreting the history of ureilites, which show evidence for the presence of both C and S during their formation.

A fundamental conclusion from our data is that the effect of C can be quite different from the effect from other non-metals, such as S. Thus, the presence of C in a metallic system can create a unique elemental fractionation pattern, and interpreting these patterns offers the opportunity to gain insight into the evolution of planetary bodies.

Acknowledgments

We thank D.H. Hill at the University of Arizona for etching two experiments with Nital and providing photographs. We also thank K.J. Domanik and M.J. Drake at the University of Arizona and T.J. McCoy at the Smithsonian Institution National Museum of Natural History for electron microprobe use and assistance. W.F. McDonough is thanked for providing us with his kamacite/cohenite partitioning data for Canyon Diablo. For insight into Greek, we thank D.A. Papanastassiou. The incorporation of comments from reviews by J.I. Goldstein, D. Walker, P.H. Warren, and Associate Editor G.F. Herzog improved the final manuscript, and we thank the reviewers for their time and effort. This work was supported by NASA Grants NAG5-12831 and NNG05GN04G to N.L.C., NSF Grant EAR-0330591 to A.J.C., NASA RTOP 344-31-20-18 to J.H.J, NASA Grants NAG5-13133 and NNG05GB81G to M.H., and NASA Grant NAG5-11122 to R.P. Harvey.

Associate editor: Gregory F. Herzog

Table A1
Results from previous partitioning studies in the Fe–Ni–C system

Reference	Run #	Temperature (°C)	wt% C (liq.)	*D*(Au)	*D*(Cr)	*D*(Cu)	*D*(Ge)	*D*(Ir)	*D*(Ni)	*D*(W)
Willis and Goldstein (1982)	1	1304	3.1				1.13 ± 0.04		1.19 ± 0.04	
Willis and Goldstein (1982)	2	1292	3.2				1.28 ± 0.10		1.20 ± 0.05	
Willis and Goldstein (1982)	3	1406	1.9				0.90 ± 0.03		1.03 ± 0.02	
Willis and Goldstein (1982)	4	1347	2.5				0.94 ± 0.06		1.05 ± 0.03	
Willis and Goldstein (1982)	5	1206	3.8				1.36 ± 0.17		1.28 ± 0.08	
Willis and Goldstein (1982)	6	1352	2.5	0.75 ± 0.05					1.06 ± 0.02	
Willis and Goldstein (1982)	7	1350	2.5			1.05 ± 0.03			1.07 ± 0.02	
Willis and Goldstein (1982)	8	1349	2.5		0.64 ± 0.11				1.11 ± 0.06	
Willis and Goldstein (1982)	9	1390	2.1					2.5 ± 1.2	1.02 ± 0.02	
Willis and Goldstein (1982)	10	1304	3.1					2.46 ± 0.28	1.23 ± 0.05	
Willis and Goldstein (1982)	11	1207	3.8					4.12 ± 0.68	1.38 ± 0.11	
Jones and Goodrich (1989)	40	1200	3.8	2.1						
Jones and Goodrich (1989)	44	1200	3.8					7.5		
Jones and Goodrich (1989)	46	1300	3.1				1.3			
Jones and Goodrich (1989)	47	1300	3.1	1.1						
Jones and Goodrich (1989)	51	1200	3.8	1.8						
Jones and Goodrich (1989)	53	1200	3.8				1.9			
Jones and Goodrich (1989)	55	1200	3.8				1.8			
Jones and Goodrich (1989)	56	1200	3.8					7.6		
Jones and Goodrich (1989)	58	1300	3.1				1.13			
Jones and Goodrich (1989)	59	1300	3.1					5.8		
Lauer and Jones (1999)	R17	1248	3.6						1.26	0.35
Lauer and Jones (1999)	R9	1258	3.5						1.25	0.38
Lauer and Jones (1999)	R2	1275	3.3						1.23	0.35
Lauer and Jones (1999)	R14	1283	3.3						1.20	0.41
Lauer and Jones (1999)	R13	1300	3.1						1.18	0.43
Lauer and Jones (1999)	R3	1350	2.5						1.15	0.42
Lauer and Jones (1999)	R11	1366	2.3						1.07	0.57
Lauer and Jones (1999)	R6	1450	1.4						1.04	1.38

All C contents were estimated based on the run temperature and the Fe–C phase diagram. Willis and Goldstein (1982) errors are ±1 SD. Jones and Goodrich (1989) and Lauer and Jones (1999) are abstracts, which discuss the experiments but do not provide quantitative analysis numbers. J. H. Jones and H. V. Lauer Jr. provided the specific numbers for these experiments.

Appendix A. Previous Fe–Ni–C experimental partitioning data

Experimental solid/liquid partition coefficients from the three previous 1 atm studies conducted in the Fe–Ni–C system (Willis and Goldstein, 1982; Jones and Goodrich, 1989; Lauer and Jones, 1999) are tabulated below. All partition coefficients are given as wt% ratios, as detailed in Eq. (1). To provide consistency for comparison between the different studies, all of the C contents listed in Table A1 were determined based on the reported run temperatures and the Fe–C phase diagram (Okamoto, 1990), as was done for our experimental results reported in Tables 1 and 2.

References

Brandon, A.D., Walker, R.J., 2005. The debate over core–mantle interaction. *Earth Planet. Sci. Lett.* **232**, 211–225.

Brandon, A.D., Walker, R.J., Morgan, J.W., Norman, M.D., Prichard, H.M., 1998. Coupled ^{186}Os and ^{187}Os evidence for core–mantle interaction. *Science* **280**, 1570–1573.

Brandon, A.D., Norman, M.D., Walker, R.J., Morgan, J.W., 1999. ^{186}Os–^{187}Os systematics of Hawaiian picrites. *Earth Planet. Sci. Lett.* **174**, 25–42.

Brandon, A.D., Walker, R.J., Puchtel, I.S., Becker, H., Humayun, M., Revillon, S., 2003. ^{186}Os–^{187}Os systematics of Gorgona Island komatiites: implications for early growth of the inner core. *Earth Planet. Sci. Lett.* **206**, 411–426.

Buchwald, V.F., 1975. *Handbook of Iron Meteorites*, vol. 1. University of California Press, Berkeley.

Campbell, A.J., Humayun, M., 1999a. Trace element microanalysis in iron meteorites by laser ablation ICPMS. *Anal. Chem.* **71**, 939–946.

Campbell, A.J., Humayun, M., 1999b. Microanalysis of platinum group elements in iron meteorites using laser ablation ICP-MS. In: *Lunar and Planet. Sci. XXX*. Abstract #1974. Lunar and Planetary Institute, Houston (CD-ROM).

Campbell, A.J., Humayun, M., Weisberg, M.K., 2002. Siderophile element constraints on the formation of metal in the metal-rich chondrites Bencubbin, Weatherford, and Gujba. *Geochim. Cosmochim. Acta* **66**, 647–660.

Chabot, N.L., Agee, C.B., 2003. Core formation in the Earth and Moon: new experimental constraints from V, Cr, and Mn. *Geochim. Cosmochim. Acta* **67**, 2077–2091.

Chabot, N.L., Jones, J.H., 2003. The parameterization of solid metal–liquid metal partitioning of siderophile elements. *Meteorit. Planet. Sci.* **38**, 1425–1436.

Chabot, N.L., Campbell, A.J., Jones, J.H., Humayun, M., Agee, C.B., 2003. An experimental test of Henry's Law in solid metal–liquid metal systems with implications for iron meteorites. *Meteorit. Planet. Sci.* **38**, 181–196.

Chabot, N.L., Draper, D.S., Agee, C.B., 2005. Conditions of core formation in the Earth: constraints from Nickel and Cobalt partitioning. *Geochim. Cosmochim. Acta* **69**, 2141–2151.

Elliott, R.P., 1965. *Constitution of Binary Alloys*. McGraw-Hill, New York, first supplement.

Gessmann, C.K., Rubie, D.C., 2000. The origin of the depletions of V, Cr, and Mn in the mantles of the Earth and Moon. *Earth Planet. Sci. Lett.* **184**, 95–107.

Goodrich, C.A., 1992. Ureilites: a critical review. *Meteoritics* **27**, 327–352.

Greenwood, N.N., Earnshaw, A., 1984. *Chemistry of the Elements*. Pergamon Press, New York.

Hansen, M., 1958. *Constitution of Binary Alloys*. McGraw-Hill Book Company, New York.

Hillgren, V.J., Gessmann, C.K., Li, J., 2000. An experimental perspective on the light element in Earth's core. In: Canup, R.M., Righter, K. (Eds.), *Origin of the Earth and Moon*. The University of Arizona Press, Tucson, pp. 245–263.

Humayun, M., Rushmer, T., Rankenburg, K., Brandon, A.D., 2005. A model for siderophile element distribution in planetary differentiation. In: *Lunar and Planet. Sci. XXXVI*. Abstract #2208. Lunar and Planetary Institute, Houston (CD-ROM).

Jana, D., Walker, D., 1997. The impact of carbon on element distribution during core formation. *Geochim. Cosmochim. Acta* **61**, 2759–2763.

Jeanloz, R., 1990. The nature of the Earth's core. *Annu. Rev. Earth Planet. Sci.* **18**, 357–386.

Jones, J.H., Drake, M.J., 1983. Experimental investigations of trace element fractionation in iron meteorites, II: the influence of sulfur. *Geochim. Cosmochim. Acta* **47**, 1199–1209.

Jones, J.H., Goodrich, C.A., 1989. Siderophile trace element partitioning in the Fe–Ni–C system: preliminary results with application to ureilite petrogenesis. *Meteoritics* **24**, 281–282.

Jones, J.H., Malvin, D.J., 1990. A nonmetal interaction model for the segregation of trace metals during solidification of Fe–Ni–S, Fe–Ni–P, and Fe–Ni–S–P alloys. *Metall. Trans. B* **21B**, 697–706.

Kallemeyn, G.W., Warren, P.H., 2005. Siderophile geochemistry of ureilites: reading the record of early stages of planetesimal core formation. In: *Lunar and Planet. Sci. XXXVI*. Abstract #2165. Lunar and Planetary Institute, Houston (CD-ROM).

Kleine, T., Munker, C., Mezger, K., Palme, H., 2002. Rapid accretion and early core formation on asteroids and the terrestrial planets from Hf-W chronometry. *Nature* **418**, 952–955.

Labrosse, S., Poirier, J.-P., Le Mouël, J.-L., 2001. The age of the inner core. *Earth Planet. Sci. Lett.* **190**, 111–123.

Lauer, H.V., Jones, J.H., 1999. Tungsten and Nickel partitioning between solid and liquid metal; implications for high-pressure metal/silicate experiments. In: *Lunar and Planet. Sci. XXX*. Abstract #1617, Lunar and Planetary Institute, Houston (CD-ROM).

Li, J., Agee, C.B., 2001. The effect of pressure, temperature, oxygen fugacity and composition on partitioning of nickel and cobalt between liquid Fe–Ni–S alloy and liquid silicate: implications for the Earth's core formation. *Geochim. Cosmochim. Acta* **65**, 1821–1832.

McDonough, W.F., Horn, I., Lange, D., Rudnick, R.L., 1999. Distribution of platinum group elements between phases in iron meteorites. In: *Lunar and Planet. Sci. XXX*. Abstract #2062, Lunar and Planetary Institute, Houston (CD-ROM).

Meibom, A., Frei, R., 2002. Evidence for an ancient osmium isotopic reservoir in Earth. *Science* **296**, 516–518.

Moffatt, W.G., 1986. *Handbook of Binary Phase Diagrams*, vol. II. Genium Publishing, Schenectady, NY.

Okamoto, H., 1990. C–Fe (Carbon–Iron), second ed.. In: Massalski, T.B. (Ed.), *Binary Alloy Phase Diagrams*, vol. 1 ASM International, pp. 842–848.

Puchtel, I.S., Brandon, A.D., Humayun, M., Walker, R.J., 2005. Evidence for the early differentiation of the core from Pt–Re–Os isotope systematics of 2.8 Ga komatiites. *Earth Planet. Sci. Lett.* **237**, 118–134.

Raghavan, V., 1988. *Phase Diagrams of Ternary Iron Alloys*, vol. 2. Indian National Scientific Documentation Centre, New Delhi, India.

Raynor, G.V., Rivlin, V.G., 1988. *Phase Equilibria in Iron Ternary Alloys*, vol. 4. The Institute of Metals, London.

Righter, K., Drake, M.J., 1999. Effect of water on metal–silicate partitioning of siderophile elements: a high pressure and temperature terrestrial magma ocean and core formation. *Earth Planet. Sci. Lett.* **171**, 383–399.

Righter, K., Drake, M.J., Yaxley, G., 1997. Prediction of siderophile element metal/silicate partition coefficients to 20 GPa and 2800 °C: the effects of pressure, temperature, oxygen fugacity and silicate and metallic melt compositions. *Phys. Earth Planet. Int.* **100**, 115–134.

Schoenberg, R., Kamber, B.S., Collerson, K.D., Eugster, O., 2002. New W-isotope evidence for rapid terrestrial accretion and very early core formation. *Geochim. Cosmochim. Acta* **66**, 3151–3160.

Selle, J.E., 1974. Binary Phase Diagram Chart. In: Lynch, C.T. (Ed.), *Handbook of Materials Science, vol. I: General Properties*. CRC Press, Cleveland, Ohio, USA, pp. 662–664.

Schersten, A., Elliott, T., Hawkesworth, C., Norman, M., 2004. Tungsten isotope evidence that mantle plumes contain no contribution from the Earth's core. *Nature* **427**, 234–237.

Walker, D., 2000. Core participation in mantle geochemistry: Geochemical Society Ingerson Lecture, GSA Denver, October 1999. *Geochim. Cosmochim. Acta* **64**, 2897–2911.

Walker, R.J., Morgan, J.W., Horan, M.F., 1995. Osmium-187 enrichment in some plumes: evidence for core–mantle interaction? *Science* **269**, 819–822.

Walker, R.J., Morgan, J.W., Beary, E.S., Smoliar, M.I., Czamanske, G.K., Horan, M.F., 1997. Applications of the ^{190}Pt–^{186}Os isotope system to geochemistry and cosmochemistry. *Geochim. Cosmochim. Acta* **61**, 4799–4807.

Walter, M.J., Thibault, Y., 1995. Partitioning of tungsten and molybdenum between metallic liquid and silicate melt. *Science* **270**, 1186–1189.

Willis, J., Goldstein, J.I., 1982. The effects of C, P, and S on trace element partitioning during solidification in Fe–Ni alloys. In: Proc. Lunar Planet. Sci. Conf. 13th. Part I. *J. Geophys. Res.* **87**, *Supplement*, A435–A445.

Wood, B.J., 1993. Carbon in the core. *Earth Planet. Sci. Lett.* **117**, 593–607.

Yin, Q., Jacobsen, S.B., Yamashita, K., Blichert-Toft, J., Telouk, P., Albarede, F., 2002. A short timescale for terrestrial planet formation from Hf-W chronometry of meteorites. *Nature* **418**, 949–952.